Coherent Terahertz Emission of Intrinsic Josephson Junction Stacks in the Hot Spot Regime

H. B. Wang,[1] S. Guénon,[2] B. Gross,[2] J. Yuan,[1] Z. G. Jiang,[3] Y. Y. Zhong,[3] M. Grünzweig,[2] A. Iishi,[1] P. H. Wu,[3] T. Hatano,[1] D. Koelle,[2] and R. Kleiner[2]

[1]*National Institute for Materials Science, Tsukuba 3050047, Japan*

[2]*Physikalisches Institut-Experimentalphysik II and Center for Collective Quantum Phenomena, Universität Tübingen, Auf der Morgenstelle 14, D-72076 Tübingen, Germany*

[3]*Research Institute of Superconductor Electronics, Nanjing University, Nanjing 210093, China*

(Received 15 April 2010; published 28 July 2010; publisher error corrected 28 July 2010)

We report on THz emission measurements and low temperature scanning laser imaging of $Bi_2Sr_2CaCu_2O_8$ intrinsic Josephson junction stacks. Coherent emission is observed at large dc input power, where a hot spot and a standing wave, formed in the ''cold'' part of the stack, coexist. By changing bias current and bath temperature, the emission frequency can be varied by more than 40%; the variation matches the Josephson-frequency variation with voltage. The linewidth of radiation is much smaller than expected from a purely cavity-induced synchronization. Thus, an additional mechanism seems to play a role. Some scenarios, related to the presence of the hot spot, are discussed.

DOI: 10.1103/PhysRevLett.105.057002 PACS numbers: 74.50.+r, 74.72.−h, 85.25.Cp

Phase synchronization is one of the prerequisites to use Josephson junction arrays as tunable high frequency sources [1–4]. While Nb based junctions are limited to frequencies below 1 THz—with applications up to 600 GHz [5]—intrinsic Josephson junctions (IJJs) [6,7] in $Bi_2Sr_2CaCu_2O_8$ are, at least in principle, able to operate up to several THz. Stacks of many junctions can be made, e.g., by patterning mesa structures on top of single crystals. For many years, investigations focused on small structures consisting of some 10 IJJs, with lateral sizes of a few μm. Here, with few exceptions [8,9], the IJJs in the stack tended to oscillate out-of-phase or were not synchronized at all. Experimental and theoretical studies included the generation of synchronous Josephson oscillations by moving Josephson vortices [8–13], the use of shunting elements [14–16], the excitation of Josephson plasma oscillations via heavy quasiparticle injection [17,18] or the investigation of stimulated emission due to quantum cascade processes [19]. High-frequency emission of unsynchronized intrinsic junctions has been observed up to 0.5 THz [20]. For more details, see Ref. [2].

Recently, coherent off-chip THz radiation with an extrapolated output power of some μW was observed from stacks of more than 600 IJJs, with lateral dimensions in the 100 μm range [21–25]. Phase synchronization involved a cavity resonance oscillating along the short side of the mesa. This radiation was studied theoretically in a series of recent papers, either based on vortex-type or plasmonic excitations, coupled to cavity modes [26–36], or on nonequilibrium effects caused by quasiparticle injection [37].

While THz emission was obtained at relatively low bias currents and moderate dc power input [21–25], using low temperature scanning laser microscopy (LTSLM) we have shown that standing wave patterns, presumably associated with THz radiation, can be obtained at high input power where, in addition, a hot spot (i.e., a region heated to above the critical temperature T_c) forms within the mesa structure [38]. Hot spot and waves seem to be correlated. The purpose of the present work is to investigate THz emission in this high power regime in detail, combining THz emission measurements and LTSLM. Apart from further clarifying the role of the hotspot, we are specifically interested in the question whether *coherent* radiation can be achieved in spite of the high temperatures involved.

By photolithogaphy and ion milling, 330×50 μm^2 large mesa structures were patterned on top of $Bi_2Sr_2CaCu_2O_8$ single crystals [39]. Below we discuss two samples, with thicknesses of 1 μm (sample 1) and 0.7 μm (sample 2), corresponding to stacks of, respectively, 670 and 470 IJJs. Mesa and base crystal were contacted by Au wires fixed with silver paste. Insulating polyimide was used to surround the mesa edge at which an Au wire was attached. In order to provide a load line for stable operation, the mesas were biased using a current source and variable resistor in parallel to the mesa. Contact resistances (around 5 Ω) are subtracted in the data discussed below. THz emission measurements were performed in Tsukuba; the samples were subsequently shipped to Tübingen for LTSLM. In total we detected THz emission from seven (out of a total of twelve) mesas on five different crystals. In one case (sample 1) emission was detected both at low bias and in the (high bias) hot spot regime; a disk shaped sample [40] radiated close to the hot spot nucleation point. Five others radiated in the hot spot regime only. Thus, the hot spot, although not a necessary ingredient for THz emission, seems to help considerably in increasing the yield of radiating samples.

The LTSLM setup is described in Ref. [38]. In brief, the laser beam is scanned across the sample surface. Local heating by 2–3 K in an area of a few μm^2 and about 0.5 μm in depth causes a change ΔV of the voltage V across the mesa serving as the contrast for the LTSLM

image. Standing waves can be imaged due to the beam-induced local change of the quality factor, leading to a strong signal ΔV at antinodes and a weak signal at nodes, located at the mesa edge, if ΔV is dominated by the magnetic field. The edge of a hot spot leads to a strong signal, while ΔV is small in the interior of the hot spot and in the "cold" part of the mesa [38]. The THz emission setup, allowing for bolometric detection and Fourier spectrometry, is described in detail in Ref. [39]. We note that numbers quoted below refer to *detected* power, to be extrapolated to 4π using the 0.04 sr aperture of the setup.

We first discuss THz emission data of sample 1, measured at $T = 20$ K. Figure 1(a) shows by solid circles the current voltage characteristic (IVC), as measured in Tsukuba. Starting from zero current, groups of junctions become resistive for $I > 20$ mA. At $I = 30$ mA the whole stack switches to the resistive state. Lowering the bias in this state the IVC is continuous down to ~10 mA where another switch to a current of ~8 mA occurs. As revealed by LTSLM, this switch corresponds to the disappearance of the hot spot present at high bias. For 3 mA $< I <$ 10 mA the IVC is continuous until further switches and hystereses appear due to the retrapping to the zero voltage state of some of the IJJs in the stack. Note that, due to different environmental noise, the switching currents to the resistive state differ for the two IVCs. However, the outermost branch, which is of interest here, nearly coincides for both IVCs, allowing for a fair, although not perfect, comparison of LTSLM and emission measurements. Figures 1(b) and 1(c) show the emission power detected by the bolometer as a function of, respectively, I and V. The largest response occurs in the high power (hot spot) regime and covers a current range from 10 mA up to ~30 mA. Here, V ranges from 0.83 to 1.13 V. If all N IJJs in the stack are *frequency* locked and participate in radiation we expect that the Josephson relation $V/N = \Phi_0 f$ holds, where Φ_0 is the flux quantum and f is the emission frequency. The Fourier spectrum, at given bias, revealed a single sharp emission line (with a resolution limited $\Delta f \approx 12$ GHz linewidth) continuously shifting with V. Two spectra are shown in Fig. 1(d). From these data we infer $N = 676 \pm 5$ in very good agreement with the 1 μm thickness of the mesa. The maximum detected power was 6 nW, corresponding to roughly 2 μW when extrapolating to 4π, even without taking additional losses into account. Thus the emitted power is comparable to the one quoted in Ref. [21]. Sample 1 also showed a bolometric response at low bias [c.f., grey (orange) lines in Figs. 1(b) and 1(c)]. Here, the detected power (~0.4 nW) was too low for Fourier spectrometry.

The different peaks visible in the radiometer data of Figs. 1(b) and 1(c) are likely to correspond to different cavity modes excited in the mesa (a similar case is shown in Fig. 3 of Ref. [38]). For the present sample, only for a bias at the main emission peak the standing wave pattern appeared. Figure 1(e) shows five LTSLM images at the bias points indicated in Fig. 1(b). The bright circular feature visible in the left part of the mesa is the hot spot. In all

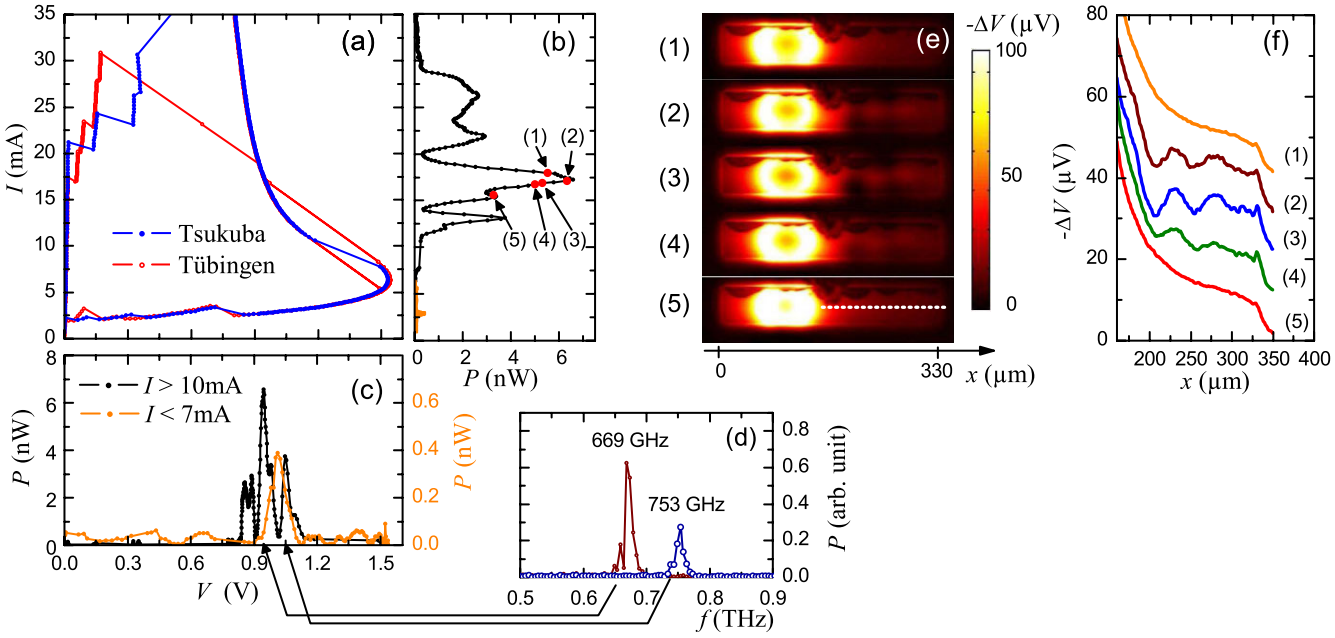

FIG. 1 (color online). Sample 1 at $T = 20$ K: IVCs (a) as measured in Tsukuba and in Tübingen. Emission power detected by the bolometer vs current (b) and voltage (c) at high bias ($I > 10$ mA) and low bias ($I < 7$ mA). Arrows labeled (1) to (5) indicate bias points of LTSLM images in (e). Fourier spectra (d) of emitted radiation taken at $V = 944$ mV, $I = 17.2$ mA (peak at 669 GHz), and $V = 1046$ mV, $I = 13.2$ mA (peak at 753 GHz). LTSLM images (e) and corresponding line scans (f) at the bias points indicated in (b). Line scans, taken along the center of the mesa, are shown only for the "cold" part of the mesa, c.f., dashed line in image (5) of graph (e). Adjacent line scans are vertically offset by 10 μV.

images there is a wavy dark feature at the upper edge of the mesa; this is caused by the polyimide covering the mesa edge. While, apart from the polyimide feature, LTSLM images (1) and (5) are smooth in the right part of the mesa, in images (2), (3), and (4) a wavy feature can be seen which is strongest along the center of the junction. Line scans in Fig. 1(f), taken in the right part of the mesa along the dashed line indicated in graph (5) of Fig. 1(e), show the wave feature in more detail. Maximum modulation is observed at bias point (3) which is close to the center of the main emission peak. Away from this bias, the wave amplitude decreases and becomes undetectable at bias points (1) and (5). This indicates a clear correlation between waves and emission. LTSLM did not reveal standing wave features outside the main emission peak (e.g., at the secondary emission peaks between 20 and 30 mA). However, this should not be interpreted as emission without waves, since, by experience, it is more difficult to see signals of waves than, e.g., of hot spots in LTSLM.

LTSLM images (2), (3), and (4) indicate that a standing wave, consisting of a half wave along the mesa width and about three half waves along its length, has been excited. From our data we infer wavelengths $\lambda_x \approx \lambda_y \approx 100\ \mu$m. Using $f = c(\lambda_x^{-2} + \lambda_y^{-2})^{1/2}$, with $f = 0.67$ THz, we find a mode velocity $c \approx 4.7 \times 10^7$ m/s, which is fully compatible with the *in-phase* mode velocity at the elevated temperatures (60–70 K) estimated for the cold part of the mesa [38,41]. Other (collective) mode velocities are by a factor of at least 2 lower. If the junctions would oscillate incoherently, the relevant mode velocity is the Swihart velocity $\bar{c} \approx 3 \cdot 10^5$ m/s, which is even lower. We thus conclude that all junctions oscillate in-phase.

We next discuss emission data of sample 2. IVCs, the bolometric response and Fourier spectrometer data are shown in Fig. 2. The largest emission was detected near a voltage of 456 mV [c.f., Figs. 2(b) and 2(c)]. Figure 2(d) shows Fourier spectra at $V = 440$ mV and $V = 451$ mV. From the emission peaks at, respectively, 531 and 554 GHz, we find the Josephson relation $V/N = \Phi_0 f$ to hold, with $N \approx 400$ (i.e., somewhat less than the 470 junctions expected from the mesa thickness). The 16 GHz linewidth is at the resolution limit. LTSLM revealed that a hot spot formed for $I > 25$ mA, covering about half of the mesa area for the bias where maximum emission was detected (increasing the current from 40 to 60 mA, the length of the cold part of the mesa decreased from about 200 to 150 μm). A standing wave pattern was vaguely visible, however, further analysis of the LTSLM data was prevented by a spurious strong response, presumably caused by additional IJJs switching to the resistive state when illuminated by the laser. Figure 3 shows emission data taken at different bath temperatures. The frequency range of detectable emission is shown in Fig. 3(a). Radiation was found between 15 and 58 K, with a maximum detected output power of about 5.5 nW near $T =$ 50 K [c.f., Fig. 3(b)]. At the lower temperatures, the emission frequencies varied continuously between 600 GHz and about 750 GHz; with increasing bath temperature the frequency of maximum emission power decreased, to about 450 GHz near 55 K; also, the frequency tunability by bias current decreased with increasing bath temperature, but still was on the order of 10% at 50 K. In the "low bias" case, the cavity resonance frequency is essentially fixed by the geometry of the mesa and may or may not be met by the frequency of the Josephson oscillations, set by the voltage V/N across each junction. In the hot spot regime (where V/N decreases with increasing bias current and bath temperature) the situation becomes more flexible (although, still, resonance is not possible for all cases).

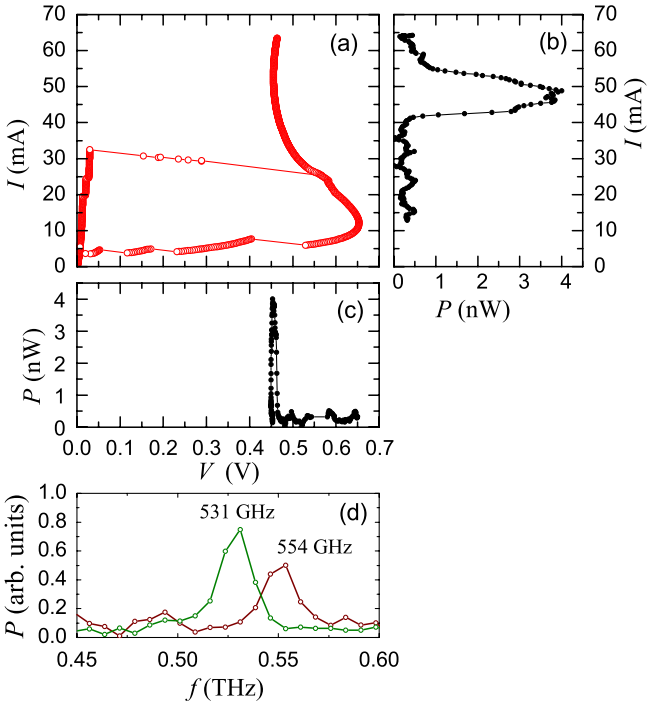

FIG. 2 (color online). Sample 2 at $T = 40$ K: IVCs (a), emission power vs current (b), and voltage (c). Panel (d) shows two spectra of the emitted power at $V = 440$ mV (peak at 531 GHz) and $V = 451$ mV (peak at 554 GHz).

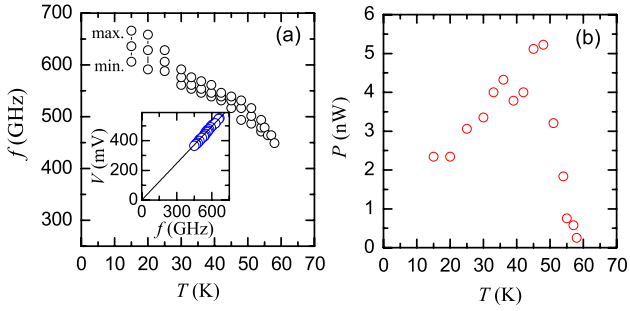

FIG. 3 (color online). Range of emission frequencies f (a) and detected emission power (b) of sample 2 vs bath temperature. Inset in (a) shows the voltage across the mesa as a function of f. Solid line in the inset is function $V = Nf\Phi_0$, with $N = 400$.

There are two factors contributing to this. First, the mode velocity c_1 decreases with increasing dc input power [38]. For example, at $T = 40$ K, over the resonance peak the input power varied from 18 to 26 mW; over such a range, at high temperatures, c_1 can decrease by some 20%–30%. Second, the hot spot changes the length L_c of the cold part of the mesa (at $T = 40$ K L_c changed by about 30% over the emission peak). Which of the two effects dominates depends on the effective temperature of the cold part and on the mode excited. In any case, the possibility to achieve resonance conditions over a comparatively wide frequency range allowed to test the Josephson relation $V/N = \Phi_0 f$, which we found to hold for all bias currents and temperatures, with $N = 400$ [c.f., inset of Fig. 3(a)].

The above results may show that, as in the low bias regime, also at high bias cavity modes are important for synchronizing the Josephson currents. However, there might be additional ingredients. For sample 1, the (resolution limited) 12 GHz linewidth of radiation is more than 50 times smaller than the oscillation frequency. For sample 2, $\Delta f/f < 0.03$ at $T = 40$ K. If, in the hot spot regime, Δf were determined by the quality factor Q of the cavity, one would require a $Q = f/\Delta f$ of at least 30–50. For a high Q cavity one would expect that clear resonant current steps are visible on the IVC which is not the case. For reference, one may analyze the IVCs of small-sized, few-junction stacks. For $T \approx 60$–70 K, these IVCs are only weakly hysteretic and Q is well below 10. The same will hold for the large mesas. One option for additional synchronization is that the hot spot interior effectively acts as a synchronizing element (*RC* or *RLC* shunt) [16,36,41,42]; another option is that (nonequilibrium) phenomena, in the spirit of Refs. [17–19,37], taking place at the hot spot edge, help in synchronizing the junctions, eventually leading to the small values of Δf observed. The fact that the Josephson-frequency-voltage relation holds rules out a purely quasiparticle related process, however, should not contradict a scenario of interacting Josephson and quasiparticle currents.

In summary, we have investigated THz emissison from intrinsic Josephson junction stacks by off-chip emission measurements and by low temperature scanning laser imaging. The stacks emit radiation coherently at high input power where a hot spot has formed. Here, standing wave patterns are observed pointing to the importance of cavity resonances for synchronization. By changing the mode velocity c_1, as well as the size of the cold part of the mesa, the hot spot allows one to vary the resonance frequency of the cavity. The linewidth of radiation, however, is too small to be determined by the cavity alone, pointing to an additional mechanism of synchronization.

We thank A. Yurgens, V. M. Krasnov, U. Welp, L. Ozyuzer, K. Kadowaki, I. Iguchi, K. Nakajima, and C. Otani for valuable discussions. Financial support by the JST/DFG strategic Japanese-German International Cooperative Program, and Grants-in-Aid for scientific research from JSPS is gratefully acknowledged.

[1] M. Darula, T. Doderer, and S. Beuven, Supercond. Sci. Technol. **12**, R1 (1999).
[2] X. Hu and S. Z. Lin, Supercond. Sci. Technol. **23**, 053001 (2010).
[3] F. Song *et al.*, Appl. Phys. Lett. **95**, 172501 (2009).
[4] I. Ottaviani *et al.*, Phys. Rev. B **80**, 174518 (2009).
[5] V. P. Koshelets and S. Shitov, Supercond. Sci. Technol. **13**, R53 (2000).
[6] R. Kleiner *et al.*, Phys. Rev. Lett. **68**, 2394 (1992).
[7] A. A. Yurgens, Supercond. Sci. Technol. **13**, R85 (2000).
[8] T. Clauss *et al.*, Appl. Phys. Lett. **85**, 3166 (2004).
[9] S. O. Katterwe and V. M. Krasnov, Phys. Rev. B **80**, 020502 (2009).
[10] R. Kleiner, Phys. Rev. B **50**, 6919 (1994).
[11] A. V. Ustinov and S. Sakai, Appl. Phys. Lett. **73**, 686 (1998).
[12] M. Machida *et al.*, Physica C (Amsterdam) **330**, 85 (2000).
[13] H. B. Wang *et al.*, Appl. Phys. Lett. **89**, 252506 (2006).
[14] H. B. Wang *et al.*, Appl. Phys. Lett. **77**, 1017 (2000).
[15] S. Madsen, G. Filatrella, and N. F. Pedersen, Eur. Phys. J. B **40**, 209 (2004).
[16] A. Grib and P. Seidel, Phys. Stat. Sol. (RRL) **3**, 302 (2009).
[17] K. Lee *et al.*, Phys. Rev. B **61**, 3616 (2000).
[18] E. Kume, I. Iguchi, and H. Takahashi, Appl. Phys. Lett. **75**, 2809 (1999).
[19] V. M. Krasnov, Phys. Rev. Lett. **97**, 257003 (2006).
[20] I. Batov *et al.*, Appl. Phys. Lett. **88**, 262504 (2006).
[21] L. Ozyuzer *et al.*, Science **318**, 1291 (2007).
[22] K. Kadowaki *et al.*, Physica C (Amsterdam) **468**, 634 (2008).
[23] L. Ozyuzer *et al.*, Supercond. Sci. Technol. **22**, 114009 (2009).
[24] H. Minami *et al.*, Appl. Phys. Lett. **95**, 232511 (2009).
[25] K. Kadowaki *et al.*, J. Phys. Soc. Jpn. **79**, 023703 (2010).
[26] L. N. Bulaevskii and A. E. Koshelev, Phys. Rev. Lett. **99**, 057002 (2007).
[27] A. E. Koshelev and L. N. Bulaevskii, Phys. Rev. B **77**, 014530 (2008).
[28] S. Lin and X. Hu, Phys. Rev. Lett. **100**, 247006 (2008).
[29] A. E. Koshelev, Phys. Rev. B **78**, 174509 (2008).
[30] X. Hu and S. Z. Lin, Phys. Rev. B **80**, 064516 (2009).
[31] R. A. Klemm and K. Kadowaki, arXiv:0908.4104.
[32] Y. Nonomura, Phys. Rev. B **80**, 140506 (2009).
[33] M. Tachiki, S. Fukuya, and T. Koyama, Phys. Rev. Lett. **102**, 127002 (2009).
[34] T. Koyama *et al.*, Phys. Rev. B **79**, 104522 (2009).
[35] S. Savel'ev *et al.*, Rep. Prog. Phys. **73**, 026501 (2010).
[36] N. Pedersen and S. Madsen, IEEE Trans. Appl. Supercond. **19**, 726 (2009).
[37] V. M. Krasnov, Phys. Rev. Lett. **103**, 227002 (2009).
[38] H. B. Wang *et al.*, Phys. Rev. Lett. **102**, 017006 (2009).
[39] See supplementary material at http://link.aps.org/supplemental/10.1103/PhysRevLett.105.057002 for details of sample preparation and the THz emission setup.
[40] S. Guénon *et al.*, arXiv:1005.2341.
[41] A. A. Yurgens (unpublished).
[42] M. Tachiki (unpublished).